Jurnal Sains Kesihatan Malaysia **6** (1) 2008: 35-60

Brain Activations Evoked by Passive and Active Listening: A Preliminary Study on Multiple Subjects

(Pengaktifan Otak yang Dicetus oleh Pendengaran Pasif dan Aktif: Satu Kajian Permulaan ke Atas Subjek Berbilang)

AHMAD NAZLIM YUSOFF, MAZLYFARINA MOHAMAD, MOHD MAHADIR AYOB & MOHD HARITH HASHIM

ABSTRACT

A functional magnetic resonance imaging (fMRI) study was conducted on 4 healthy male and female subjects to investigate brain activation during passive and active listening. Two different experimental conditions were separately used in this study. The first condition requires the subjects to listen to a simple arithmetic instruction (e.g. one-plus-two-plus-three-plus-four) – passive listening. In the second condition, the subjects were given the same series of arithmetic instruction and were required to listen and perform the calculation – active listening. The data were then analysed using the Statistical Parametric Mapping (SPM5) and the MATLAB 7.4 (R2007a) programming softwares. The results obtained from the fixed (FFX) and random effects analyses (RFX) show that the active-state signal intensity was significantly higher ($p < 0.05$) than the resting-state signal intensity for both conditions. The results also indicate significant differences ($p < 0.001$) in brain activation between passive and active listening. The activated cortical regions during passive listening, as obtained from the FFX of the first condition is symmetrical in the left and right temporal and frontal lobes covering the cortical auditory areas. However, for the second condition, which was active listening, more activation occurs in the left hemisphere with a reduction in the number of activated voxels and their signal intensity in the right hemisphere. Activation mainly occurs in the middle temporal gyrus, precentral gyrus, middle frontal gyrus, superior temporal gyrus and several other areas in the frontal lobes. The point of maximum signal intensity has been shifted to a new coordinates during active listening. It is also observed that the magnetic resonance signal intensity and the number of activated voxel in the right and left superior temporal lobes for the second condition have been reduced as compared to that of the first condition. The results obtained strongly suggest the existence of functional specialisation. The results also indicate different networks for the two conditions. These networks clearly pertain to the existence of functional

connectivity between activation areas during listening and listening while performing a simple arithmetic task.

Key words: Fixed effects analysis (FFX), Random effects analysis (RFX), Functional magnetic resonance imaging (fMRI), Statistical parametric mapping (SPM), Active listening, Passive listening

ABSTRAK

Kajian pengimejan resonans magnet kefungsian (fMRI) telah dijalankan ke atas 4 orang subjek lelaki dan wanita sihat untuk menyelidiki pengaktifan otak semasa pendengaran pasif dan aktif. Dua keadaan uji kaji yang berbeza digunakan secara berasingan dalam kajian ini. Keadaan pertama memerlukan subjek mendengar arahan aritmetik mudah (cth. satu-campur-dua-campur-tiga-campur-empat) – pendengaran pasif. Dalam keadaan kedua, subjek diberikan siri arahan aritmetik yang sama dan diminta mendengar dan melakukan pengiraan – pendengaran aktif. Data kemudiannya dianalisis menggunakan pakej perisian pemetaan statistik berparameter (SPM5) dan MATLAB 7.4 (R2007a). Keputusan yang diperolehi daripada Analisis Kesan Malar (FFX) dan Kesan Rawak (RFX) menunjukkan bahawa keamatan isyarat keadaan aktif adalah lebih tinggi secara bererti ($p < 0.05$) berbanding keamatan isyarat keadaan rehat untuk kedua-dua keadaan. Keputusan juga menunjukkan perbezaan pengkhususan kefungsian yang bererti ($p < 0.001$) dalam pengaktifan otak di antara pendengaran pasif dan aktif. Kawasan korteks yang aktif semasa pendengaran pasif, seperti yang diperolehi daripada FFX keadaan pertama berlaku secara simetri pada lobus temporal dan frontal merangkumi kawasan korteks auditori. Walau bagaimanapun, untuk keadaan kedua, iaitu pendengaran aktif, lebih banyak pengaktifan berlaku pada hemisfera kiri dengan pengurangan dalam bilangan dan keamatan isyarat voksel aktif pada hemisfera kanan. Pengaktifan berlaku terutamanya pada girus temporal tengah, girus presentral, girus frontal tengah, girus temporal superior dan beberapa kawasan lain pada lobus frontal. Titik dengan keamatan isyarat maksimum telah teranjak ke koordinat baru semasa pendengaran aktif. Dapat diperhatikan juga bahawa keamatan isyarat resonans magnet dan bilangan voksel aktif pada lobus superior temporal kanan dan kiri telah dikurangkan jika dibandingkan dengan keadaan pertama. Keputusan yang diperolehi mencadangkan kewujudan pengkhususan kefungsian. Keputusan juga menunjukkan rangkaian yang berbeza untuk kedua-dua keadaan. Rangkaian ini menunjukkan dengan jelas kewujudan kehubungan kefungsian di antara kawasan pengaktifan semasa mendengar dan mendengar sambil melakukan tugasan aritmetik mudah.

Kata kunci: Analisis kesan malar (FFX), Analisis kesan rawak (RFX), Pengimejan resonans magnet kefungsian (fMRI), Pemetaan

statistik berparameter (SPM), Pendengaran aktif, Pendengaran pasif

INTRODUCTION

The emergence of several new techniques in studying how human brain works, in particular, positron emission tomography (PET), functional magnetic resonance imaging (fMRI) along with the event related potentials (ERPs) obtained from electroencephalography (EEG) or magnetoencephalography (MEG) in the past 20 years has significantly escalated the growth in the number of studies conducted in the field of cognitive neuroscience. Until today, this research area is continuously expanding because of much recent prominence in the advancement in medical imaging technologies and the existence of clusters of collaboration of researchers from different institutions and backgrounds that have put their mind together into this and had moulded the area of cognitive neuroscience more integrative in nature. The underlying objectives in imaging neuroscience as proposed by Friston (2004) are mainly to identify specialised functional areas (the analyses of regionally specific effects : which area constitute a neuronal system) and to determine the integrative function among specific areas (analyses of inter-regional effects: what are the interactions between the elements of a given neuronal system). The latter can then be divided into two specific objectives which are commonly referred to as functional connectivity (determination of the temporal correlation between spatially remote neurophysiological events) and effective connectivity (determination of the influence that the elements of a neuronal system exert over another). The most common imaging technique used among imaging neuroscience communities in exploring the structure and function of human brain with regard to functional specialisation and integration is fMRI (Turner 1995; Amaro and Barker 2006).

fMRI is one of the many advanced applications of magnetic resonance imaging (MRI) in which anatomical brain structures and the corresponding part of the brain that participate in specific neurological functions can be precisely located and simultaneously studied (Buxton 2002). It is well known that fMRI examination can be conducted noninvasively, in the sense that it neither uses ionising radiation nor radioactive tracers to produce images. It is also known that fMRI examination does not need exogenous contrast media to be administered into the subjects for image enhancement. Nevertheless, this imaging modality can provide imaging neuroscientists with high resolution brain images together with the activations and in any preferable directions namely axial, coronal, sagittal and even in oblique slice orientations. The ability of fMRI in detecting small metabolic changes in the brain lies on the state-of-the-art of an imaging technique or pulse sequence invented by Mansfield, the Echo Planar Imaging (EPI) (Mansfield 1977 and Bernstein et al. 2004) and the discovery of a remarkable

endogenous contrast agent, the oxyhemoglobin, by Ogawa et al. (1990a and 1990b) and Ogawa and Lee (1990). The invention of EPI and the discovery of oxyhemoglobin as an endogenous contrast agent, hence Blood Oxygenation Level Dependent (BOLD), since then had shed lights on a vast number of studies in functional neuroimaging. Activations in the brain due to various physical (motor, auditory and visual), psychological (memory, learning and attention) and physiological (in response to drugs or inhaled gasses) stimuli can be clearly observed and studied using fMRI. Consequently, these have led to compilations of fMRI data sets into databases in many imaging neuroscience centers and had made the production of the maps of human brain functions possible. All these efforts would then benefit the clinicians especially in diagnosing the function or wellness of any particular part of the healthy or deceased brain before performing treatment or surgery.

In this work, the height (signal intensity) and spatial (activation area) extent of brain activations due to passive and active listening in four healthy male and female subjects are studied by means of the fMRI technique and statistical parametric mapping (SPM) method. The individual, group fixed and random effects analyses are performed on both sets of functional data and statistical inferences are made on the basis of Gaussian random field theory (RFT) controlled by the family-wise error rate, taking $p < 0.05$ as significant. These analyses were based on the consideration that neighboring voxels are nonconservative in nature. Finally, the results obtained are compared and conclusions are drawn with regard to functional specialisation of the activated areas and functional connectivity among the regions of interest (ROI) that pertain to passive and active listening. To date, local mechanisms underlying the change in the intensity of the BOLD signal and the extent of the area covered by the activation in human cortical systems evoked by simple arithmetic–based tasks has not been fully understood and need more attention (Nair 2005). A comprehensive multiple subjects study in this area is needed to better understand the functional and structural cortical connections that mediate human perception to word numbers and their interaction with higher language and cognitive function, i.e. solving simple arithmetic tasks, in the brain, stimulated using auditory stimuli. This can certainly be accomplished by combining the noninvasive nature of fMRI examination and statistically based parametric mapping of human brain function (SPM).

EXPERIMENTAL METHODS

SUBJECT

Functional magnetic resonance imaging (fMRI) examinations were performed on four healthy male and female subjects. The subjects were paid and given informed consent and screening forms as required by the Research and Medical Research Ethical Committee of the Universiti Kebangsaan Malaysia (UKM) – Reference

Number FF-205-2006. The subjects were interviewed on their health condition prior to the scanning session and were confirmed to be healthy. Prior to the fMRI scans, the subjects' middle ear condition and hearing level (HL) were measured in the Department of Audiology and Speech Sciences UKM via a timpanometer (Model Grason Stadler GSI33) and an audiometer (Model Grason Stadler GSI61) respectively. The middle ear condition and hearing level in the frequency range of 250 – 8000 Hz for all subjects were found to be normal (HL < 20 dB). The subjects were also told not to move their head during the scan. Changes in signal intensity over time from any one voxel can arise from head motion as well as due to the existence of serial correlations and drift and these would certainly represents a serious confound particularly in fMRI studies (Friston 2004). The immobilising devices were used together with the head coil in order to minimise head movement. Demographical data for all the subjects are depicted in Table 1.

TABLE 1. Demographical data for all subjects

Subject	Gender	Race	Age	Handedness	Middle ear condition	Hearing level	
						R	L
N1	Male	Malay	25	Right	normal	< 20 dB	< 20 dB
N2	Male	Malay	25	Right	normal	< 20 dB	< 20 dB
N3	Male	Malay	36	Right	normal	< 20 dB	< 20 dB
N4	Female	Malay	23	Right	normal	< 20 dB	< 20 dB

MRI SCANS

Functional magnetic resonance imaging (fMRI) examinations were conducted in the Department of Radiology, Universiti Kebangsaan Malaysia Hospital (Ahmad Nazlim Yusoff et al. 2005). Functional images were acquired using a 1.5 T magnetic resonance imaging (MRI) system (Siemens Magnetom Vision VB33G) equipped with functional imaging option, echo planar imaging (EPI) capabilities and a radiofrequency (RF) head coil used for signal transmission and reception. Gradient Echo – Echo Planar Imaging (GRE-EPI) pulse sequence with the following parameters were applied: Repetition time (TR) = 1 ms, echo time (TE) = 66 ms, field of view (FOV) = 210 × 210 mm, flip angle (α) = 90°, matrix size = 128 × 128 and slice thickness = 4 mm. Using the midsagittal scout image (TR = 15 ms, TE = 6 ms, FOV = 300 × 300 mm, α = 30°, matrix size = 128 × 128 and magnetic field gradient = 15 mT/m) produced earlier, 35 axial slice positions (1 mm interslice gap) were oriented in the anterior-posterior commissure (AC-PC) plane. This covers the whole brain volume. In addition, high resolution anatomical images of the entire brain were obtained using a strongly T1-weighted spin echo pulse sequence with the following parameters: TR = 1000 ms, TE = 30 ms, FOV = 210 × 210 mm, α = 90°, matrix size = 128 × 128 and slice thickness = 4 mm.

EXPERIMENTAL PARADIGM

The subjects were given detail instructions on how to response to the given stimuli prior to the scanning. Two sets of functional scans which use the GRE-EPI pulse sequence were consecutively conducted on the subjects. In the first functional scan, the subjects were instructed to listen to a series of simple mental arithmetic tasks (i.e. 1 + 2 + 3 + 4) verbally given via a headphone which is connected to a personal computer (PC) – passive listening. In the second scan, the subjects were required to perform the calculation as they listen to a similar task – active listening. The PC setup is equipped with a soundcard with 24-bit ADVANCED HD™ USB Sound System (USB Sound Blaster Audigy 2NX). The mathematical instructions were given by the text-to-speech translation programme installed in the PC using Microsoft Sam as the computer's default voice. A six-cycle active-rest paradigm which was alternately cued between active and rest was used with each cycle consists of 10 series of measurements during active state and 10 series of mesurements during resting state. Both the passive and active listening tasks were given during the active states. Each functional measurement produces 20 axial slices in 3 s (one image slice in 150 ms). The measurement started with active state. The imaging time for each functional scan is 360 s (6 minutes) which produces $120 \times 20 = 2400$ images in total. A high resolution T2* weighted images are obtained using the voxel size of $1.64\,\text{mm} \times 1.64\,\text{mm} \times 4.00\,\text{mm}$.

POST PROCESSING OF THE fMRI DATA

All the functional (T2*-weighted) and structural (T1-weighted) images were sent to Universiti Kebangsaan Malaysia Hospital (HUKM) MedWeb and were later retrieved in the Functional Image Processing Laboratory, Diagnostic Imaging & Radiotherapy Programme, Faculty of Allied Health Sciences, UKM Kuala Lumpur for further analyses. Image analyses were performed using a personal computer (PC) with a high processing speed and large data storage. The MATLAB 7.4 – R2007a (Mathworks Inc., Natick, MA, USA) and Statistical Parametric Mapping (SPM5) (Functional Imaging Laboratory, Wellcome Department of Imaging Neuroscience, Institute of Neurology, University College of London) software packages were used for that purposes. The raw data in DICOM (.dcm) format were transformed into Analyze (.hdr, .img) format by means of SPM5. Functional images in each measurement were realigned using a 6-parameter affine transformation in translational (x, y and z) and rotational (pitch, roll and yaw) directions to reduce artifacts from subject movement and in order to make within and between subject comparison a meaningful way. In the process (Ashburner & Good 2003), a reference image (the first image of a measurement serie) is chosen and remain stationary in space. The other images (source images) are than spatially transformed to match the reference image. A mapping is

determined from each voxel position in the reference to a corresponding position in the source image. The source images are then resampled at the estimated position. The images were then time-correct using sinc interpolation to ensure that each measurement is subjected to the same time interval. After realigning the data, a mean image of the series is used to estimate some warping parameters that map it onto a template that already conforms to a standard anatomical space (EPI template provided by the Montreal Neurological Institute – MNI) (Friston 2004). The complexity and variability of human brain across subjects is so great that reliance on maps and atlases (such as construction of averages, templates and models) is essential to manipulate, analyse and interpret brain data effectively (Toga and Thomson 2000). The normalisation procedure used a 12-parameter affine transformation where the parameters constitute a spatial transformation matrix (Ashburner & Friston 2004). The images were then smoothed using a 6-mm full-width-at-half-maximum (FWHM) Gaussian kernel. Activated voxels were identified by the general linear model approach by estimating the parameters of the model and by deriving the appropriate test statistic (*T* statistic) at every voxel. Statistical inferences were finally obtained on the basis of SPM and the Gaussian random field theory (Friston 2004). Steps taken in data analyses using SPM have been completely described in Ahmad Nazlim Yusoff et al. (2006a, 2006b, 2006c).

RESULTS AND DISCUSSION

In a standard functional neuroimaging analysis, a statistical model is usually fit to the data by means of the general linear model as shown by Fig. 1(a). The model explains the data in terms of a linear combination of the explanatory variables (B1 and B2) plus an error term (ε). The model in matrix notation can be written as $Y = X\beta + \varepsilon$ where Y is the column vector of observations, ε the column vector of error terms and β the column vector of parameters β_1 and β_2, see Fig. 1(b). X is the designed matrix of dimension (J, 2) which contains the effects that influenced the measured signal, for example signals from the active and rest states in the passive and active listening experiments respectively. Y is also referred to as the measured time series data of length J at a given location (voxel) in the brain. In this study, J or the number of measurement conducted on each particular subject is 120 (Ahmad Nazlim Yusoff et al. 2006b and 2006c). The model parameters (β_1 and β_2) are then determined by means of the least square fitting method to look for any effect such as the difference between active and rest states. In doing that, a statistic for each brain voxel that tests for the effect of interest in that voxel is calculated, resulting in a large volume of statistic for the whole brain volume. One now has to decide whether this volume shows any evidence of the effect. To achieve this, an independent *t*-test is conducted between data collected during the active and rest states and the *t* values obtained is compared to the null distribution for the *t* statistic, see Brett et al. (2004).

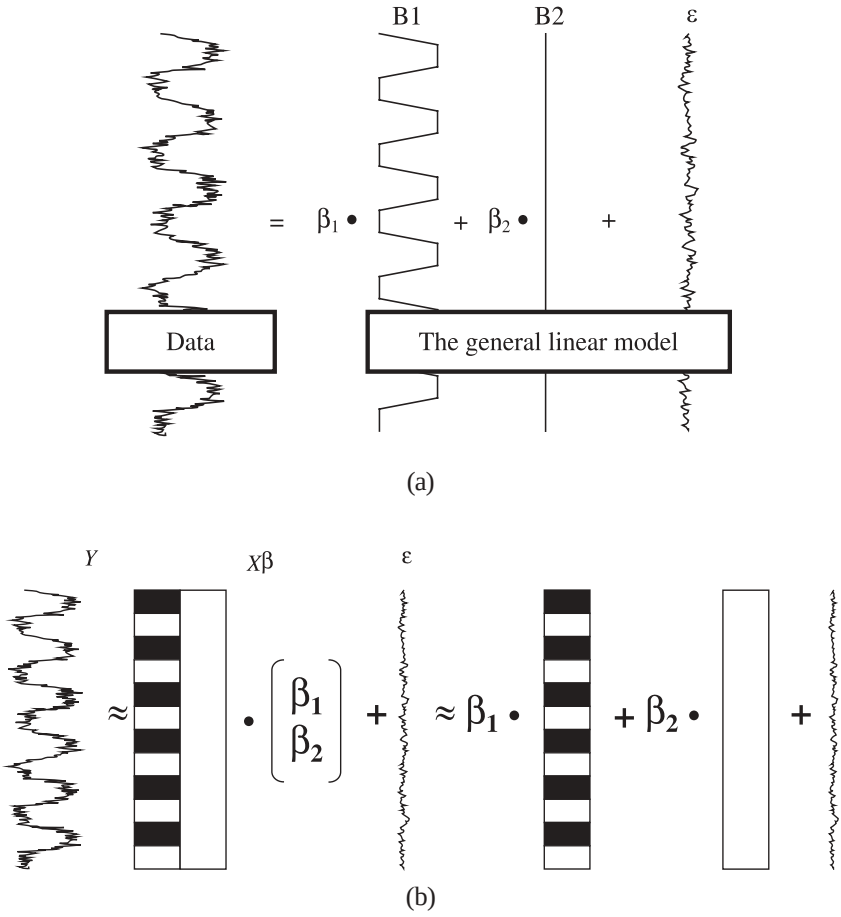

FIGURE 1. (a) The general linear model representing the measured data and (b) its matrix notation

In SPM, the *t* value for each time series voxel for the *T*-contrast image is calculated from the relation (Poline et al. 2004)

$$t = [c^{T}\beta]/[\sqrt{\text{var}[c^{T}\beta]}]. \quad (1)$$

Eqn. (1) can also be written as

$$t = [c^{T}\beta]/[\sigma(c^{T}(X^{T}X)^{-1}c)^{1/2}] \quad (2)$$

where c is the weight of the parameter estimates used to form the numerator of the statistics, c^{T} is the transposed matrix of c, β is the parameter model to be

estimated (i.e. β_1 and β_2), σ is the standard deviation and X and X^T is the designed matrix and its transposition respectively. The parameter c is actually a vector or matrix that contains the contrasts weights. In other words, the t value is the contrast of the estimated parameters or the effect size, $c^T\beta$, divided by the square root of the variance estimate which is var[$c^T\beta$]. The contrast weights must be specified to define the contrast. The shadowed regions or blobs on the statistical parametric maps (shown in Figs. 3 and 4), hence, represent the statistical image of the effects of interest, for example the activated brain areas during the passive or active listening experiments. The results are obtained from the application of t-test (T contrast) on each voxel and by taking the p value smaller than a designated alpha (α) value as significant. In other words, for a given voxel, the general linear model, by means of least square fitting, will figure out just what type that voxel is by modeling it as a linear combination of the hypothetical time series, as discussed earlier and in Ahmad Nazlim Yusoff et al. (2006c). The fitting or estimation entails finding the parameter values (β_1 and β_2) such that the linear combination best fits the measured data. These conclude that the same general linear model can be used for all voxels but with different set of parameters for each voxel.

A simple extension of the model in Fig. 1(a) and (b) for an individual subject is given in design matrix representation in Fig. 2(a). The main condition (active and rest) is now modeled with three basis functions namely the canonical hemodynamic response function (HRF) and its temporal and dispersion derivatives. The peristimulus basis set of the canonical HRF and its derivatives are depicted next to the design matrix. These functions are able to model the HRF as well as its delay and dispersion. The temporal derivative has been shown to be able to capture differences in the latency of the peak response while the dispersion derivative determines the duration of the peak response (Henson 2004). These three basis functions are convolved with the statistical model used when fitting the model with the data for each voxel. The design matrix is accompanied (on the top) by the selected contrasts which were chosen to produce the effects of passive or active listening that can be obtained from the whole experiment. A detail discussion on contrast and classical inference has been given by Poline et al. (2004). Specifically, the first column of the design matrix modeled the hemodynamic response for the active and rest states for either passive or active listening respectively. The second and third columns represent the time and dispersion derivatives of the canonical HRF. The fourth to ninth columns modeled the movement related artifacts in both translational and rotational directions. The rationale in modeling the movement related artifacts is to compensate for imperfect motion correction in both directions during realignment. The final or the tenth column is dedicated to the global. To test for any activation due to passive or active listening with the exclusion of the effects from the derivatives and movement related responses, the matrix c^T is taken as [1 0 0 0 0 0 0 0 0 0], as shown in Fig. 2(a). By taking this contrast, SPM will calculate the difference in signal intensity between the active and resting states for each voxel without any inteference from other effects.

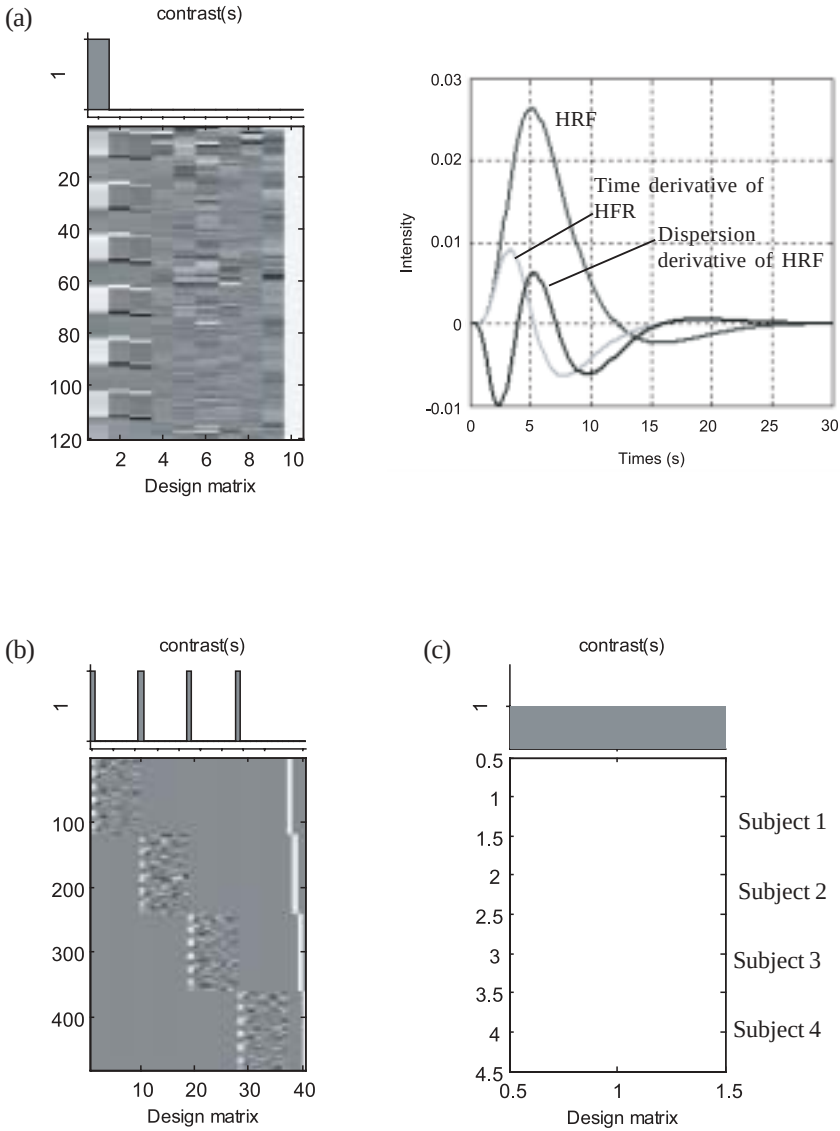

FIGURE 2. Design matrix used in data analysis for (a) individual, (b) fixed and (c) random effects analyses. Also shown in (a) are the canonical HRF together with its time and dispersion derivatives

The statistical analyses done in this study were based on a body of mathematics defining theoretical results for smoothed statistical maps called the random field theory (RFT) (Brett et al. 2004). Brett explained that, since there are many voxels and therefore many statistical values that are accounted for in the analyses (i.e. a statistic value for each voxel) and the hypothesis is referred to the whole volume of statistics in the brain, evidence against the null hypothesis would be that the whole observed volume of values is unlikely to have arisen from a null distribution. Due to this volume or family of voxel statistics, the risk of error that might occur is the Family-Wise Error (FWE) rate which is the likelihood that this family of voxel values could have arisen by chance. This family wise null hypothesis is tested by looking for any voxels that have statistic values larger than what are expected if they all had come from a null distribution. This method requires finding a threshold to apply to every statistic value so that any value above the threshold is unlikely to have occurred by chance. With the a value taken as 0.05 in this study, one false positive map is expected to arise in 20 statistical parametric maps. In this case, the null hypothesis which is the hypothesis that there is no effect can be rejected with a 5% risk of type I error. This 5% is also called type I error rate or the chance that we take that we are wrong when we reject the null hypothesis.

Figs. 3 (a – d) represent the glass images or the maximum intensity projection (MIP) of the brain in neurological appearance (the left side of the image is the actual left side of the brain) for individual subject showing the activations (blobs or dark regions) that exist during passive listening. The glass images shown in Fig. 3 (e) represent results obtained from statistical inference made on all subjects by means of fixed effects analysis (FFX) while Fig. 3 (f) are results derived from random effects analysis (RFX). Figs. 4 (a – f) represent results obtained using similar analyses on active listening. FFX considers the 480-volume acquisition from the four subjects as independent observations while ignoring serial correlation between acquisitions when making inference. In short, the error variance in FFX is estimated on scan-to-scan basis. The design matrix used for FFX is as shown in Fig. 2(b) with the contrast taken as [1 0 0 0 0 0 0 0 0 1 0 0 0 0 0 0 0 0 1 0 0 0 0 0 0 0 0 1 0 0 0 0 0 0 0 0 1 0 0 0 0 0 0 0 0 0]. The inference in RFX on the other hand is made by considering the variability in activation effects by assessing it from subject to subject. In another words, in the individual subject analysis, the data analysed are the 120 scan-volumes whereas for the FFX, the data are the combination of the scan volume for all subjects. For the RFX, the number of sample is the number of subject in this study, which is 4. Fig. 2(c) shows the design matrix for the RFX analysis. The contrast used is [1].

The glass images or better named as statistical images in Figs. 3 (a – f) and Figs. 4 (a – f) obtained from the individual analysis, FFX and RFX were generated via the statistical parametric mapping (SPM5) analysis on each voxel using the *T*-contrast or SPM{T}. The results were projected onto the Tailairach and Tournoux stereotactic coordinates (Tailarach and Tournoux 1988). The arrows represent

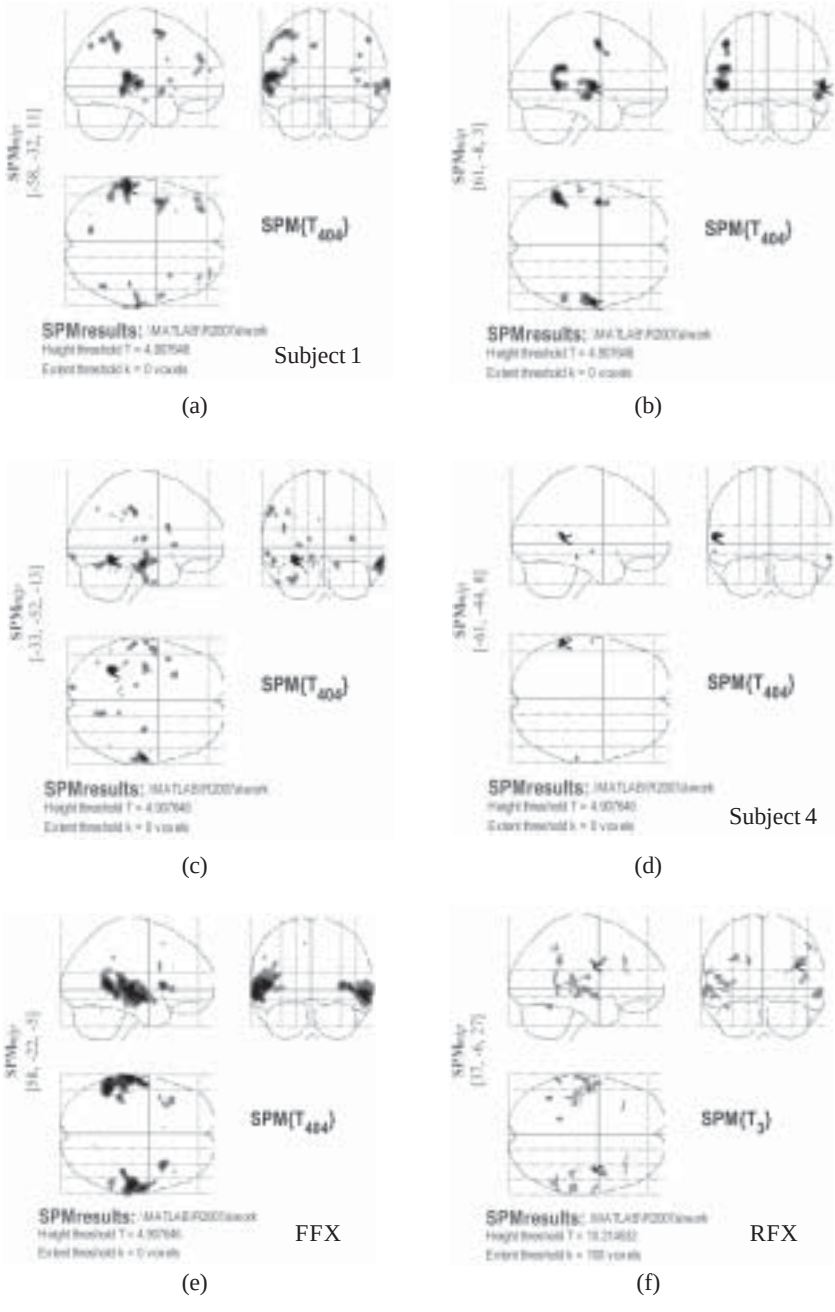

FIGURE 3. Statistical *T*-contrast images for passive listening obtained from (a – d) individual, (e) FFX and (f) RFX analyses

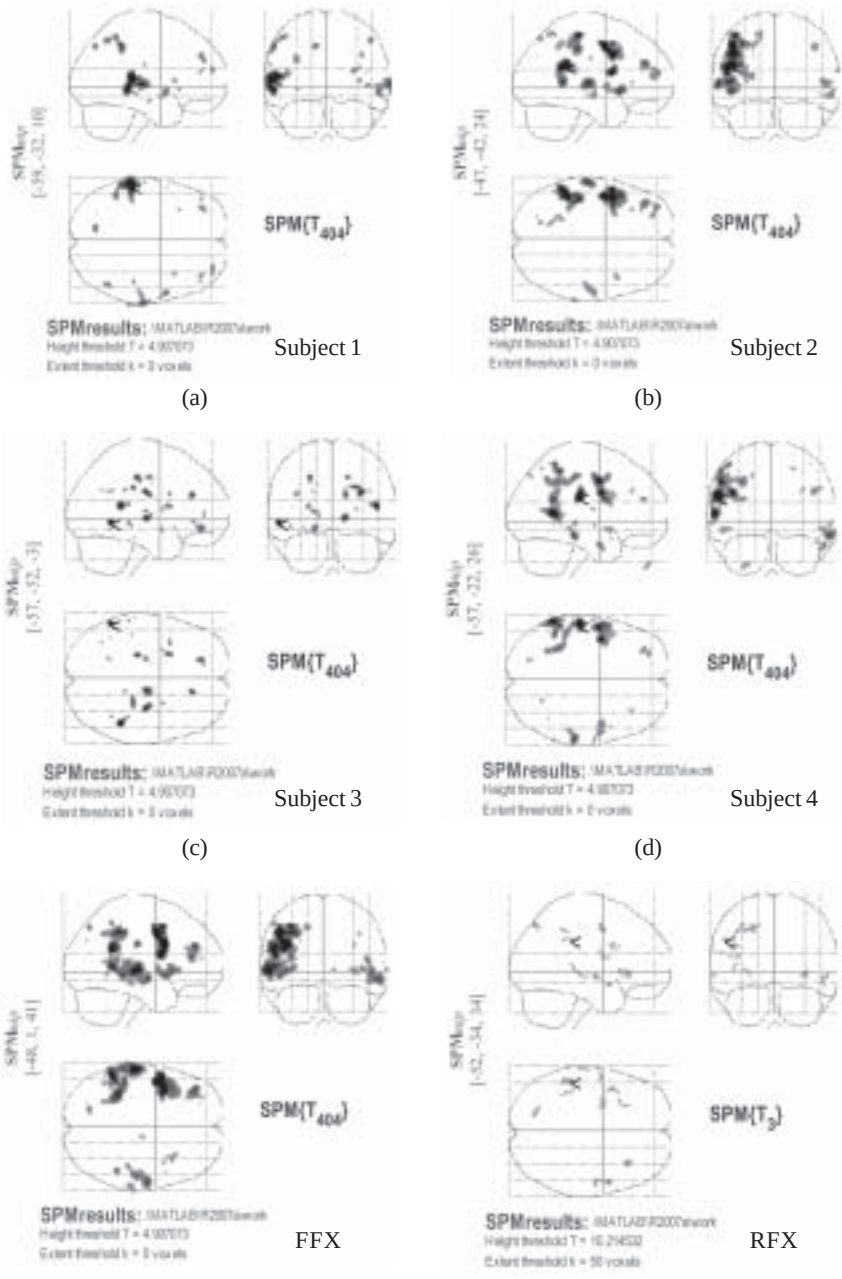

FIGURE 4. Statistical *T*-contrast images for active listening obtained from (a – d) individual (e) FFX and (f) RFX analyses

the point of maximum intensity (global maximum) in the respective analysis with the coordinates shown on the left-hand side of the figures. The darker the voxel, the higher the intensity of the BOLD signal. It is obvious that the area and signal intensity of activation obtained from individual subject are not the same. In other words, not all subjects activate a particular brain region. For example, in passive listening experiment, the auditory area is at least seemed to be activated in one of the two hemispheres in subject 1, 2 and 3 but not in subject 4. Furthermore, the subject may experience activation in many areas than others as can be seen for subject 2 in active listening experiment. The differences between the results obtained from individual analysis on all subjects clearly show the subject-specific effects which are not always the same from subject-to-subject due to the intrinsic variability in each particular subject, as can be seen in Figs. 3 (a – d) and 4 (a – d). These could be due to the difference in the BOLD signal intensity that is captured from each subject and may also arise due to subjects' different sensitivity to the stimulus given since the vasodilatory signal, cerebral blood flow (CBF), cerebral blood volume (CBV) and the quantity of deoxyhemoglobin content which govern the height and spatial extent of the activation in the brain differ significantly in individuals. The variability is thought to be intrinsic in nature since precautions in reducing the effects from confounding factors have been taken into consideration so as to assure that the experiment perform on all subjects is as similar as possible. The fact that subjects' movement in translational and rotational directions are not contributing to the observed activation is acceptable since those movement related effects have been excluded in generating the contrast images. The inferences made on each subject are only valid for that particular subject and have a variance given by

$$\sigma_w^2/n \tag{3}$$

which is equivalent to the term var[$c^T\beta$] given in Eqn. (1) with n is the number of measurements for each subject and the subscript w denote within-subject variance. These inferences are not valid for representing the whole group of subjects.

For a multiple subject study, one can always make a statistical inference on a group of subjects by combining all the data obtained from all subjects by means of FFX (Snijders 2005). Figs. 3(e) and 4(e) which are the results obtained from FFX, show the average effects in the group with the variance contains from within-subject terms only. However, the analyses now involve all the four subjects with a number of 480 scans (as compared to 120 scans for individual analysis) with the assumption that each scan represent an independent observation with no serial correlation. The variance for the FFX can be written as

$$\sigma_w^2/Nn \tag{4}$$

with N is the number of subjects in the group and n is the number of measurement for each subject. The error variance in FFX is also estimated on scan-to-scan basis but the degree of freedom in FFX is therefore the number of scans which is 480, minus the rank of the design matrix. Comparing Eqns. (3) and (4) implies that the effect size is larger and the variance is smaller for FFX than that of the individual analysis resulting in a larger *t* value that is assigned to each voxel which is truly activated by the passive and active listening stimuli. If the same height threshold is used, the resulting statistical image will have more activated voxels with higher signal intensities. With this method, FFX is able to exclude false positive voxels that are activated during individual analysis. The two statistical images in Figs. 3(e) and 4(e) can be said to be the representative statistical images of the four subjects for both passive and active listening respectively. It can be said that the mean group response embodies an activation. However, this does not constitute an inference that the group's respones is significant, for example, that this sample of subjects shows a consistent activation (Friston 2004). In other words, the FFX analysis is not suitable for making inferences about population effects but is perfectly valid for making inferences about the particular subjects studied. In order to make an inference that the group showed a significant activation, one would have to assess the variability in activation effects from subject to subject (Friston 2004).

The results depicted in Figs. 3(f) and 4(f) are that obtained from RFX analysis for both passive and active listening. The appropriate error variance in RFX is based on the activation from subject to subject where the effect per se constitutes an independent observation and the degrees of freedom fall dramatically to the number of subjects (Friston 2004). As compared to the average effects of the group obtained from FFX, fewer voxels are seemed to be significantly active. This is because RFX analysis takes into account the between-subject variability which is normaly larger than that of between scans, resulting in a smaller *t* values. The population variance for RFX can be written as

$$\sigma_b^2/N + \sigma_w^2/Nn \qquad (5)$$

with the subscript b and w denote between-subject and within subject variances. The mean activation when compared to the variability in activation from subject to subject is smaller in terms of number of voxels and intensity due to the contribution from both the within-subject and between-subject variances in RFX. This concludes that the variability between subject taken into consideration in the RFX is larger than the variability within subject for FFX (Snijders 2005). Smaller area of activation with a reduction in signal intensity might also means that more subjects are needed in order for a valid statistical conclusion to be made on a population. RFX is usually more conservative as compared to FFX. This method reflects the fact that the subjects are drawn at random from a large population, allowing the inference to be generalised to the population from

which the subjects were selected, given a proper number of subjects. RFX with simple two-sample *t*-test conducted on this group of subject revealed that there is no significant different ($p > 0.05$) in brain activation between male and female subjects and and between age group, below or above 30 years old.

Due to the small number of subjects involved in this study, the results on the height and spatial extent of brain activation obtained from RFX is thought to be insufficient to be thoroughly discussed. Therefore, the following discussion will be based on results generated by SPM by means of FFX on all subjects. Table 2 and 3 respectively show some statistical data, Talairach MNI coordinates at the point of maximum intensity in each respective cluster and the anatomical areas in which the maxima in the brain activation due to passive and active listening occur. The activated areas are anatomically interpreted using a MATLAB based SPM5 toolbox which enables the integration of the probabilistic cytoarchitectonic maps with the results generated by SPM (Eickhoff et al. 2005). As describe by Friston et al. (1996), the corrected *p* values shown in the tables are derived based on the set-level inferences (number of activated regions), cluster-level inferences (number of activated voxels) and voxel-level inferences (the *p* value for each voxel within the cluster. Friston et al. (1996) further describe that the set-level inferences refer to the inferences that the number of clusters or set of clusters comprising an observed activation profile is highly unlikely to have occurred by chance. This level of inference is based on the probability of getting the observed number of clusters or more in the volumed analysed, defined by a height and an extent threshold. In this work, by considering the family wise null hypothesis (FWE) and by taking the α value as 0.05 in the analyses of random field theory (RFT) and by performing a one-sample *t* test onto all voxels, there are six significant clusters ($p < 0.001$) that exist in the passive listening task and thirteen significant clusters ($p < 0.001$) in the active listening task, after thresholding clusters that contain less than 100 voxels. For the purpose of discussion, only eight significant clusters are shown for active listening. This is due to the fact that the other five clusters are believed to be generated by factors not included in the experimental paradigm such as aliased biorhythm and mild responses of the brain during the experiment. Cluster-level inferences, on the other hand are a special case of set-level inferences that occur when the number of clusters is assumed to be equivalent to 1. Defined by a height threshold, this procedure permit statistical inference to be made about each cluster and is based on the probability of getting a cluster of the size observed or a larger one in the volume analysed. All the number of activated voxels in the clusters determined from the SPM for both conditions are significant with $p < 0.05$. Similarly, voxel-level inferences are a special case of cluster-level inferences that result when the cluster is small. It is based on the probability that the observed voxel value or a higher one could have occurred by chance in the volume analysed. In Figs. 3(e) and 4(e), only voxels that have a significant difference in intensity between active and rest are therefore shaded. Voxel-level tests permit individual voxel to be identified as

TABLE 2. Statistical data, Tailairach coordinates (x, y, z) and the respective anatomical areas obtained from passive listening by means of FFX. Clusters with number of voxel less than 100 are thresholded

Set-level		Cluster-level		Voxel-level		*x*, *y*, *z* (mm)			Anatomical area
$P_{corrected}$	Clusters	$P_{corrected}$	No. of voxel	$P_{corrected}$	*t*-value				
< 0.001	P1	< 0.001	9034	< 0.001	8.25	58	-22	-5	Right superior temporal gyrus
				< 0.001	7.15	62	-9	-10	Right superior temporal gyrus
				< 0.001	7.04	44	-30	2	Right superior temporal gyrus
	P2	< 0.001	13354	< 0.001	8.24	-62	-23	-1	Left middle temporal gyrus
				< 0.001	8.12	-50	-48	7	Left middle temporal gyrus
				< 0.001	7.97	-63	-14	-8	Left middle temporal gyrus
	P3	< 0.001	1059	< 0.001	6.83	34	15	4	Right insula lobe
	P4	< 0.001	569	< 0.001	5.72	-39	25	1	Left inferior frontal gyrus (p. triangularis)
		< 0.001		< 0.001	5.18	-32	17	2	Left insula lobe
	P5	< 0.001	192	< 0.001	5.60	-42	11	29	Left inferior frontal gyrus (p. opercularis)
	P6	< 0.001	593	< 0.001	5.51	54	-43	7	Right middle temporal gyrus
				< 0.001	5.30	61	-43	2	Right middle temporal gyrus
				< 0.001	5.02	56	-48	-3	Right middle temporal gyrus

TABLE 3. Statistical data, Tailairach coordinates (x, y, z) and the respective anatomical areas obtained from active listening by means of FFX. Clusters with number of voxel less than 100 are thresholded. There are altogether thirteen significant clusters but only eight are shown for the purpose of discussion

Set-level		Cluster-level		Voxel-level		*x*, *y*, *z* (mm)			Anatomical area
$P_{corrected}$	Clusters	$P_{corrected}$	No. of voxel	$P_{corrected}$	*t*-value				
< 0.001	A1	< 0.001	7119	< 0.001	8.74	-48	1	41	Left precentral gyrus
				< 0.001	8.52	-42	8	30	Left precentral gyrus
				< 0.001	8.19	-54	6	19	Left inferior frontal gyrus (p. Opercularis)
	A2	< 0.001	13241	< 0.001	8.22	-60	-23	1	Left middle temporal gyrus
				< 0.001	8.21	-55	-47	24	Left supramarginal gyrus
				< 0.001	7.36	-55	-47	5	Left middle temporal gyrus
	A3	< 0.001	2046	< 0.001	6.94	-39	42	27	Left middle frontal gyrus
				< 0.001	6.41	-34	39	17	Left middle frontal gyrus
				0.002	5.60	-30	36	25	Left middle frontal gyrus
	A4	< 0.001	2706	< 0.001	6.93	59	-9	-8	Right superior temporal gyrus
				< 0.001	6.44	51	-22	-2	Right superior temporal gyrus
				< 0.001	6.05	42	-30	3	- not assigned -
	A5	< 0.001	419	< 0.001	6.92	-57	-20	30	Left postcentral gyrus
	A6	< 0.001	3310	< 0.001	6.70	-47	10	-5	Left temporal pole
				< 0.001	6.63	-40	15	0	Left insula lobe
				< 0.001	6.23	-34	20	2	- not assigned -
	A7	< 0.001	487	< 0.001	6.20	47	-42	13	Right superior temporal gyrus
				0.005	5.41	50	-42	4	Right middle temporal gyrus
	A8	< 0.001	269	< 0.001	5.96	-18	-72	47	Left superior parietal lobule

significant, whereas cluster- and set-level inferences only allow clusters or set of clusters to be declared significant.

The main activation clusters in Fig. 5 are denoted by P1, P2, P3, P4, P5 and P6 for passive listening while for active listening, the clusters are marked by A1, A2, A3, A4, A5, A6, A7 and A8. For passive listening, the maximum signal intensity in the two main clusters were found to be at coordinates (58, -22, -5) in the right superior temporal gyrus and (-62, -23, -1) in the left middle temporal gyrus in the right and left hemispheres respectively. It can be clearly seen that the area of activation is almost symmetrical in the two hemispheres during passive listening with the activation seems to be extending over the primary and secondary auditory areas, i.e. Brodmann areas 41, 22 and 42. The number of activated voxels for passive listening are 10,686 and 14,115 in the right and left hemispheres respectively, which indicates that the number of activated voxels are more than 30% higher in the later. The results for the height (BOLD intensity) extent is in consistent with that of the spatial extent (activation area) with the average signal intensity for cluster P2 is slightly higher than that of P1. The signal intensity (Singal-To-Noise Ratio – SNR) at several maxima in both main clusters (P1 and P2), are measured using SPM and the means are compared by means of the independent *t*-test using the Statistical Packages for Social Sciences (SPSS). The results indicate that the average intensity of cluster P1 is 1.21 ± 0.04 whereas for cluster P2, the average intensity is 1.25 ± 0.04 from which the difference is not significant [$p > 0.05$; CI 95% (-1.54, 0.71)] mainly due to the equality of magnitud of the BOLD signals and their variances. The results on spatial extent however, show that on average, the left auditory areas are more sensitive to the given stimuli during the binaural listening process (listening to series of numbers) conducted in this study, as compared to the right auditory areas.

For active listening, more activation occur in the left hemisphere with a reduction in the number of activated voxels and their signal intensity in the right hemisphere. Activation mainly occurs in the middle temporal gyrus, precentral gyrus, middle frontal gyrus, superior temporal gyrus and several other areas in the frontal lobes (Table 3). A number of 26,404 voxels are activated in the left hemisphere as compared to 3,193 in the right hemisphere. The point of maximum intensity during active listening occur in the left precentral gyrus with the coordinates (-48, 1, 41). When compared with passive listening, the number of activated voxel in the right superior temporal gyrus has been reduced from 9034 to 2706 but the average BOLD signal decreases insignificantly from 1.21 ± 0.04 to 1.20 ± 0.02 [$p > 0.05$; CI 95% (-0.80, 0.10)]. The change in the number of activated voxel together with the relocation of the coordinates of maximum intensity indicates that the main processing center differs in both conditions. A new network has been established during listening while performing simple arithmetic tasks. Areas A1, A3, A5 and A8 in the frontal lobe have been described to be responsible for imagination, impulsive action, thinking, planning and central

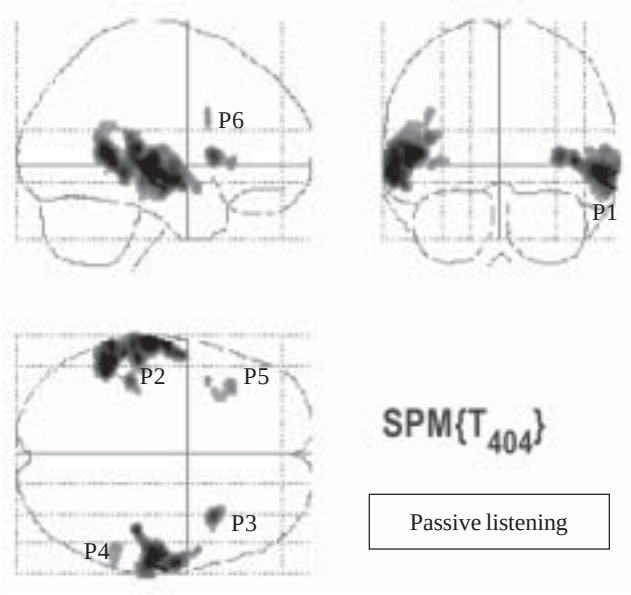

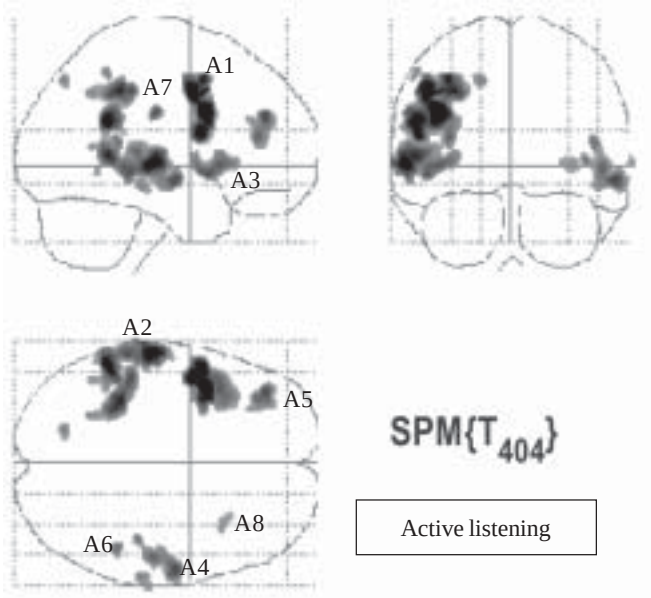

FIGURE 5. Activation clusters for passive and active listening as depicted in Table 1 and 2. The red arrows indicate the location of voxel that shows maximum signal intensity

executive functions. During active listening, the subject was instructed to perform simple arithmetic calculation when he or she hear the number sequence via a headphone. This in turn triggered neuronal firing in the respective areas in the frontal lobe, hence the occurrence of BOLD response. Arithmetic calculation includes imagination of numbers, impulsive action and thinking before the answer is finally presented by the brain. Area A2 and A4 are expected to be involved in auditory processing and general interpretive area such as for spatial arrangement of language, sounds of language and recognising word sounds, while other areas which exist during active listening but not activated during passive listening are subjected to the response of the brain when mental mathematics are presented to the subject. The fact that human brain activates its left hemisphere stronger than its right hemisphere when working on logical thinking has been proven to be true in this study.

As mentioned earlier, brain activation that occurs during passive listening is limited only to six major clusters (Table 2). These activation areas do exist during active listening task but with different distribution of area coverage and signal intensities. In this study, no activation occurs in the cerebellum as obtained in our previous study using sparse imaging fMRI (Yusoff et al. 2006). Similar to areas A2 and A4, areas P1 and P2 are designated to auditory and general interpretive processes such as for hearing, spatial arrangement of language, sounds of language and recognising word sounds and word numbers. These areas are expected to be activated since the given stimulus contains voices of a person, saying the word numbers in English language and instructing the subjects to perform the calculation. Areas P3, P4 and P5 are thought to be evoked by mathematical tasks presented to the subject. Since these areas are also activated in the active listening conditions (A5, A8 and A6) regardless of the mathematical calculation performed by the subject, these areas are also thought to be involved in recognizing word sounds and sounds of language during the presentation of tasks.

Fig. 6 shows the differential effect of passive and active listening together with the design matrix and the respective contrast used to generate the activation. The contrast used are [-1 0 0 0 0 0 0 0 0 -1 0 0 0 0 0 0 0 0 -1 0 0 0 0 0 0 0 0 -1 0 0 0 0 0 0 0 0 1 0 0 0 0 0 0 0 0 1 0 0 0 0 0 0 0 0 1 0 0 0 0 0 0 0 0 1 0 0 0 0 0 0 0 0 1 0 0 0 0 0 0 0 0]. The results show voxels that are active during active listening but do not involve in passive listening with voxels with statistics $p_{\text{uncorrected}} < 0.001$ are considered to be significant. If a higher cut-off point is used as imposed in earlier analyses on passive and active listening per se (i.e. FWE with corrected p values), there seemed to be no activation anywhere in the brain. The point of maximum intensity is now (-53, 8, 19) in the left inferior frontal gyrus which occured slightly away from the third maximum of the first cluster in active listening. It can be clearly seen that the activated voxels are all located in the left hemisphere. The results support the above discussion on the logical function of the left hemisphere.

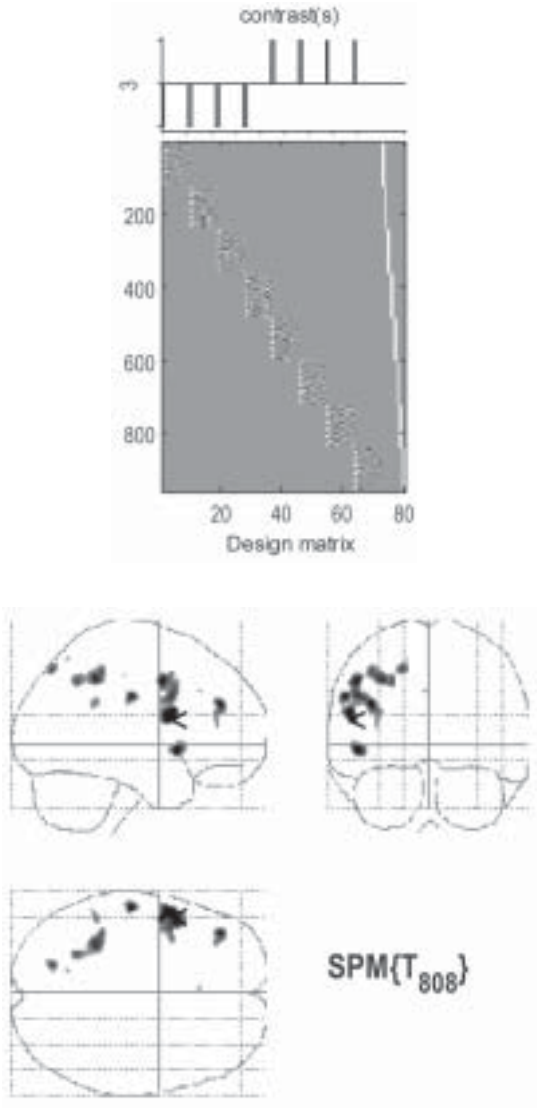

FIGURE 6. The designed matrix and contrast (top) used in the SPM analysis in looking for voxels that are active during active listening but do not take part in passive listening. Voxels with statistics ($p_{\text{uncorrected}}$) smaller than 0.001 are considered as significant (bottom)

Consequently, as Figs. 5 and 6 indicate, it can be said that the main processing center has been shifted to a new location in the brain when the subject performs the simple arithmetic task during active listening as compared to when the subject was only listening to the arithmetic instructions during passive listening. The results indicate that the brain establishes different networks for the two conditions with each of the network having different point of maximum intensity. These networks strongly suggest the existence of functional and effective connectivity between activation areas during listening and listening while performing a simple arithmetic task. Fig. 7(a) and (b) represent BOLD statistical images obtained from SPM{T} which are overlaid onto several three dimensional orientations of the subjects' average brain structure. The magnitude of the activations (the intensity of the hemodynamic response) thresholded using the *t* values are color coded indicating higher *t* values as the color changes from red to yellow. It can be clearly seen that the number of activated area increases during active listening with the distribution dominating prominently in the left hemisphere. The fact that the brain has reduced its sensitivity (height and spatial extent) in the right superior temporal gyrus during active listening is also evident from those figures. The findings in this work especially on the functional specialization, are supported by a study done by Maeder et al. (2001) who demonstrated bilateral brain activation in the posterior superior temporal lobe and inferior part of the inferior parietal lobule associated to sound recognition and localization.

The hemodynamic response function in the cerebral cortices due to the BOLD mechanism and the connectivity measure between regions of interest can be further studied and evaluated using functional magnetic resonance imaging technique and statistical parametric mapping. One of the many ways is by implementing the dynamic causal modeling (DCM) to model interactions among neuronal populations at cortical level. DCM is about the identification of nonlinear input-state-output systems. The aim is to reveal the dynamic nature of the interactions among states and to make inferences about the coupling among brain areas and how the coupling is influenced by changes in the experimental context, see Friston et al. (2003) for a complete explaination on DCM.

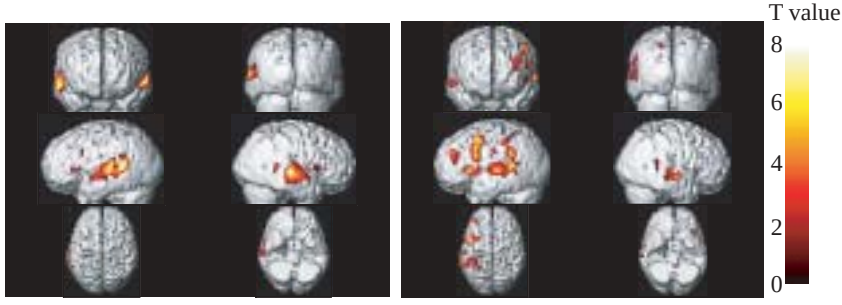

FIGURE 7. (a) BOLD statistical images obtained from SPM{T} which are overlaid onto several three dimensional orientations of the subjects' average brain structure for (a) passive and (b) active listening

CONCLUSION

In conclusion, the hemodynamic response function in the cerebral cortices due to the BOLD mechanism can be studied and evaluated using functional magnetic resonance imaging technique and statistical parametric mapping. As elaborated by Friston (2004), the implementation of the statistical analysis to make inference about the data given the effect is zero in the first-level represents a fixed effects analysis where the error variance is estimated on a scan-to-scan basis, assuming that each scan represents an independent observation (ignoring serial correlation). In other words, inference was made about the data by combining all the data obtained from the four subjects. In order to make an inference that a group of subjects showed significant activation, the variability in activation effects must be assessed from subject to subject. The variability now constitutes the proper error variance (Friston 2004). This second-level analysis is called random effects analysis in which the inference is said to be generalised to the population from which the subjects were selected. The activated cortical regions during passive listening, as obtained from the FFX of the first condition is symmetrical in the left and right temporal and parietal lobes covering the cortical auditory areas. However, for the second condition, which was active listening, brain activations were insymmetrically observed in the left and right frontal lobes, limbic lobe as well as in the left and right parietal and temporal lobes. More activations occur in the left hemisphere. The point of maximum signal intensity during passive listening has been shifted to a new coordinates during active listening. It is also observed that the magnetic resonance signal intensity and the number of activated voxel in the right and left superior temporal lobes for the second condition have been reduced as compared to that of the first condition. A further study on the response of the human brain to the passive and active listening using random effect analysis is necessary in order to make an appropriate inference about group responses. Finally, this study reveals that there exist a different network during active listening (listening while performing a simple arithmetic task) as compared to passive listening (listening to a given arithmetic task). The activation patterns in active listening seem to incorporate more cortical areas of the brain in the left hemisphere.

ACKNOWLEDGEMENT

The authors would like to thank Assoc. Prof. Dr. Siti Zamratol-Mai Sarah Mukari and Ms Nur 'Izzati Md. Yusoff, from the Department of Audiology and Speech Sciences for their kind consultations and assistances in conducting hearing tests on the subjects, the Department of Radiology, Universiti Kebangsaan Malaysia Hospital for the permission to use the MRI scanner and Profesor Karl J. Friston and the functional imaging group of the University College of London for valuable discussions on experimental methods and data analyses. This work is supported by the research grants IRPA 09-02-02-0119EA296, the Ministry of

Science, Technology and Innovation of Malaysia and and GUP-SUK-SK-07-20-205, Universiti Kebangsaan Malaysia.

REFERENCES

Ahmad Nazlim Yusoff, Mohd Harith Hashim, Mohd Mahadir Ayob & Iskandar Kassim. 2005. Pengimejan resonans magnet kefungsian: Pemerolehan, analisis dan pentafsiran data. *J. Sains Kes. Mal.* 3(2): 19-37.

Ahmad Nazlim Yusoff, Mohd Harith Hashim, Mohd Mahadir Ayob & Iskandar Kassim. 2006a. Analisis data pengimejan resonans magnet kefungsian: Pra pemprosesan ruang menggunakan kaedah pemetaan statistik berparameter. *J. Sains Kes. Mal.* 4(1): 21-36.

Ahmad Nazlim Yusoff, Mohd Harith Hashim, Mohd Mahadir Ayob, Iskandar Kassim, Nur Hartini Mohd Taib & Wan Ahmad Kamil Wan Abdullah. 2006b. Functional specialisation and connectivity in cerebral motor cortices: A single subject study using fMRI and statistical parametric mapping. *Mal. J. Med. Health Sci.* 2(2): 37-60.

Ahmad Nazlim Yusoff, Mohd Harith Hashim, Mohd Mahadir Ayob & Iskandar Kassim. 2006c. Pengaktifan otak akibat gerakan jari bagi subjek dominan tangan kanan dan kiri. *J. Sains Kes. Mal.* 4(2): 63-83.

Amaro, E. J. & Barker G. J. 2006. Study design in fMRI: Basic principles. *Brain and Cognition* 60: 220-232.

Ashburner, J. & Good, C. D. 2003 Spatial registration of images. In : P. Tofts, *Quantitative MRI of the Brain: Measuring Changes Caused by Disease*, West Sussex, England: John Wiley & Sons Ltd., 503-531.

Ashburner, J. & Friston, K. J. 2004. Computational Neuroanatomy. In : R. S. J. Frackowiak, K. J. Friston, C. D. Frith, R. J. Dolan, C. J. Price, S. Zeki, J. Ashburner and W. D. Penny (eds.), *Human Brain Function*, Amsterdam: Elsevier Academic Press, 655-672.

Bernstein, M. A., King, K. F. & Zhou, X. J. 2004. *Handbook of MRI Pulse Sequences*. Burlington: Elsevier Academic Press.

Buxton, R. B. 2002. *Introduction to Functional Magnetic Resonance Imaging: Principles and Techniques*. Cambridge: Cambridge University Press.

Brett, M., Penny, W. & Kiebel, S. 2004. An introduction to random field theory. In: R. S. J. Frackowiak, K. J. Friston, C. D. Frith, R. J. Dolan, C. J. Price, S. Zeki, J. Ashburner and W. D. Penny (eds.), *Human Brain Function*, Amsterdam: Elsevier Academic Press, 867-879.

Eickhoff, S. B., Stephan, K. E., Mohlberg, H., Grefkes, C., Fink, G. R., Amunts, K. & Zilles, K. 2005. A new SPM toolbox for combining probabilistic cytoarchitectonic maps and functional imaging data. *NeuroImage* 25: 1325-1335.

Friston, K. J., Holmes, A., Poline, J. B., Price, C. J. & Frith, C. D. 1996. Detecting activations in PET and fMRI : Levels of inference and power. *NeuroImage* 40: 223-235.

Friston, K. J. 2004. Experimental design and statistical parametric mapping. In: R. S. J. Frackowiak, K. J. Friston, C. D. Frith, R. J. Dolan, C. J. Price, S. Zeki, J. Ashburner and W. D. Penny (eds.), *Human Brain Function*, Amsterdam: Elsevier Academic Press, 599-632.

Henson, R. 2004. Analysis of fMRI time series. In: R. S. J. Frackowiak, K. J. Friston, C. D. Frith, R. J. Dolan, C. J. Price, S. Zeki, J. Ashburner & W. D. Penny (eds.), *Human Brain Function*, Amsterdam: Elsevier Academic Press, 793-822.

Friston, K. J., Harrison, L. & Penny, W. 2003. Dynamic causal modeling. *NeuroImage* 19: 1273-1302.

Maeder, P. P., Meuli, R. A., Adriani, M., Bellmann, A., Fornari, E. & Thiran, J. –P. 2001. Distinct pathways involved in sound recognition and localisation in human fMRI study. *NeuroImage* 14: 802-816.

Mansfield, P. 1977. Multiplanar image formation using NMR spin echoes. *J. Phys. C* 10: L55 – L58.

Nair, D. G. 2005. About being BOLD. *Brain Research Reviews* 50: 229-243.

Ogawa, S., Lee, T. M., Kay, A. R. & Tank, D. W. 1990a. Brain magnetic resonance imaging with contrast dependent on blood oxygenation. *Proc. Natl. Acad. Sci. U.S.A.* 87: 9868-9872.

Ogawa, S., Lee, T. M., Nayak, A. S. & Glynn, P. 1990b. Oxygenation-sensitive contrast in magnetic resonance imaging of rodent brain at high magnetic fields. *Magn. Reson. Med.* 14: 68-78.

Ogawa, S and Lee, T. M. 1990. Magnetic resonance imaging of blood vessels at high fields: in vivo and in vitro measurements and image simulation. *Magn. Reson. Med.* 16: 9-18.

Poline, J. B., Kherif, F. & Penny, W. 2004. Contrasts and Classical Inference. In : R. S. J. Frackowiak, K. J. Friston, C. D. Frith, R. J. Dolan, C. J. Price, S. Zeki, J. Ashburner and W. D. Penny (eds.), *Human Brain Function*, Amsterdam: Elsevier Academic Press, 761-779.

Snijders, T. A. B. 2005. Fixed and random effects. In B. S. Everitt and D. C. Howell (Eds.), *Encyclopedia of Statistics in Behavioural Science*, Vol. (2), Chicester: Wiley, 664-665.

Talairach, J. & Tournoux, P. 1988. *Coplanar Stereotaxic Atlas of the Human Brain*. New York: Thieme Medical.

Toga, A. W. & Thompson, P. M. 2000. An introduction to maps and atlases of the brain. In : A. W. Toga & J. C. Mazziotta (Eds.), *Brain Mapping: The Systems*, San Diego, U.S.A.: Academic Press, 3-32.

Turner, R. 1995. Functional mapping of the human brain with magnetic resonance imaging. *The Neuroscience* 7: 179-194.

Yusoff, A. N., Ayob, M. M., Hashim, M. H., Taib, N. H. M. & Mohamad, M. 2006. Brain activation in the cerebral cortices during passive and active listening: A sparse-fMRI study on a single subject. Paper presented at the 2006 Biophysics Seminar and 4th South East Asia Congress of Medical Physics (SEACOMP), 7 – 11 November, University of Indonesia, Jakarta.

Ahmad Nazlim Yusoff
Mazlyfarina Mohamad
Mohd Mahadir Ayob
Mohd Harith Hashim
Functional Image Processing Laboratory (FIPL)
Diagnostic Imaging & Radiotherapy Programme
Faculty of Allied Health Sciences
Universiti Kebangsaan Malaysia
50300 Jalan Raja Muda Abdul Aziz, Kuala Lumpur

Corresponding author: nazlimpdr@hotmail.com
Received: September 2007
Accepted for publication: January 2008